XIV CONGRESSO BRASILEIRO DE ENGENHARIA MECÂNICA

14 th BRAZILIAN CONGRESS OF MECHANICAL ENGINEERING

08 a 12 de Dezembro de 1997

December 8-12th 1997

Centro de Convenções Obeid Plaza Hotel
Bauru - SP / Brasil

ORGANIZAÇÃO

unesp

Ação conjunta:
FEG - Guaratinguetà, FEIS - Ilha Solteira,
FET - Bauru, IGCE- Rio Claro

PROMOÇÃO

ABCM
Associação Brasileira
de Ciências Mecânicas

DYNAMIC PERFORMANCE OF VARIABLE STRUCTURE HYBRID CONTROL OF MANIPULATORS

ABÍLIO AZENHA & J. A. TENREIRO MACHADO
Department of Electrical and Computer Engineering, Faculty of Engineering,
University of Porto, Rua dos Bragas, 4099 Porto Codex, Portugal
Phone: +351-2-317105, Fax: +351-2-2003610/319280,
E-mail: azenha@tom.fe.up.pt, jtm@fe.up.pt

Abstract

In this paper it is studied the implementation of a variable structure algorithm in the position/force hybrid control of robotic manipulators. The time and frequency responses of the system are calculated and its properties are studied. Moreover, the effect of the controller sampling frequency and the system stability are analysed through a linearization procedure.

Keywords

Robotics, Manufacturing Systems, Intelligent Control, Variable Structure Systems, Force Control.

1. INTRODUCTION

In the early eighties Raibert & Craig (1981) introduced the concept of force control based on the hybrid algorithm. Since then, several researchers (Khatib, 1987; Whitney, 1987; Hogan, 1985; Zhang & Paul, 1985) developed these ideas and proposed new algorithms such as the impedance controller. Problems with position/force control are further investigated in An & Hollerbach (1987) and Fisher & Mujtaba (1992), while more recent studies of this algorithm can be found in Siciliano & Villani (1996) and Volpe & Khosla (1994). Nevertheless, this area of research is only beginning to emerge from the *sea* of unexplored problems of sustained contact between the robot and the workpiece. In this line of thought, this paper presents a robust algorithm for this type of robot control that only needs a force sensor in the wrist of the arm in addition to velocity and position measurements of the joint coordinates.

The article is organised as follows. Section two introduces the position/force control algorithm. Section three shows some results with variable structure controllers (VSCs) in the position and force control loops. Section four presents the *Frequency Response* (*FR*) of the closed-loop system, while section five studies the stability of the system through a linearization. Finally, section six outlines the main conclusions.

2. THE POSITION/FORCE HYBRID CONTROLLER

The dynamic equation of an ideal rigid-link-rigid-joint robot with n links interacting with the environment is:

$$\tau = \mathbf{H}(\mathbf{q})\ddot{\mathbf{q}} + \mathbf{c}(\mathbf{q},\dot{\mathbf{q}}) + \mathbf{g}(\mathbf{q}) - \mathbf{J}^T(\mathbf{q})\mathbf{F} \tag{1}$$

Here τ is the $n \times 1$ vector of actuator torques, $\mathbf{q}$ is the $n \times 1$ vector of joint coordinates, $\mathbf{H}(\mathbf{q})$ is the $n \times n$ inertia matrix, $\mathbf{c}(\mathbf{q},\dot{\mathbf{q}})$ is the $n \times 1$ vector of centrifugal/Coriolis terms and $\mathbf{g}(\mathbf{q})$ is the $n \times 1$ vector of gravitational effects. The $n \times n$ matrix $\mathbf{J}^T(\mathbf{q})$ is the transpose of the Jacobian matrix of the robot and $\mathbf{F}$ is the $n \times 1$ vector of the force that the environment exerts in the robot end-effector.

In this study we shall adopt as prototype manipulator the 2R robot with dynamics:

$$\mathbf{H}(\mathbf{q}) = \begin{bmatrix} (m_1+m_2)r_1^2 + m_2 r_2^2 + & m_2 r_2^2 + m_2 r_1 r_2 C_2 \\ +2m_2 r_1 r_2 C_2 + J_{1m} + J_{1g} & \\ m_2 r_2^2 + m_2 r_1 r_2 C_2 & m_2 r_2^2 + J_{2m} + J_{2g} \end{bmatrix} \tag{2a}$$

$$\mathbf{c}(\mathbf{q},\dot{\mathbf{q}}) = \begin{bmatrix} -m_2 r_1 r_2 S_2 \dot{q}_2^2 - 2m_2 r_1 r_2 S_2 \dot{q}_1 \dot{q}_2 \\ m_2 r_1 r_2 S_2 \dot{q}_1^2 \end{bmatrix} \tag{2b}$$

$$\mathbf{g}(\mathbf{q}) = \begin{bmatrix} g(m_1 r_1 C_1 + m_2 r_1 C_1 + m_2 r_2 C_{12}) \\ g m_2 r_2 C_{12} \end{bmatrix} \tag{2c}$$

$$\mathbf{J}^T(\mathbf{q}) = \begin{bmatrix} -r_1 S_1 - r_2 S_{12} & r_1 C_1 + r_2 C_{12} \\ -r_2 S_{12} & r_2 C_{12} \end{bmatrix} \tag{2d}$$

where $C_i = \cos(q_i)$, $C_{ij} = \cos(q_i + q_j)$, $S_i = \sin(q_i)$, $S_{ij} = \sin(q_i + q_j)$ and a constraint plane determined by the angle θ as depicted in Fig. 1. The numerical values adopted for the ideal 2R robot are enumerated in Table 1.

Table 1: The 2R robot parameters.

i	m_i(Kg)	r_i(m)	J_{im}(Kgm^2)	J_{ig}(Kgm^2)
1	0.5	1.0	1.0	4.0
2	6.25	0.8	1.0	4.0

As usual, the contact of the robot with the constraint surface is modelled through a linear system with a mass M, a damping B and a stiffness K. The adoption of the alternative model of a dashpot with two springs (Azenha & Machado, 1997) was also investigated leading to the same kind of conclusions. The schematic structure of the position/force hybrid control algorithm is depicted in Fig. 2. The matrix $\mathbf{I}$ is the $n \times n$ identity matrix and the diagonal matrix $\mathbf{S}$ is the $n \times n$ selection matrix with elements equal to one/zero in the position/force controlled directions. In this paper we consider the y_C/x_C Cartesian coordinates to be position/force controlled according with the equations:

$$\mathbf{S}=\begin{bmatrix}0 & 0\\ 0 & 1\end{bmatrix},\ \mathbf{J}_C(\mathbf{q})=\begin{bmatrix}-r_1C_{\theta 1}-r_2C_{\theta 12} & -r_2C_{\theta 12}\\ r_1S_{\theta 1}+r_2S_{\theta 12} & r_2S_{\theta 12}\end{bmatrix},\ \Lambda_C:\ \begin{cases}x_C=r_1S_{\theta 1}+r_2S_{\theta 12}\\ y_C=r_1C_{\theta 1}+r_2C_{\theta 12}\end{cases} \tag{3}$$

where $C_{\theta 1}=\cos(\theta-q_1)$, $C_{\theta 12}=\cos(\theta-q_1-q_2)$, $S_{\theta 1}=\sin(\theta-q_1)$ and $S_{\theta 12}=\sin(\theta-q_1-q_2)$.

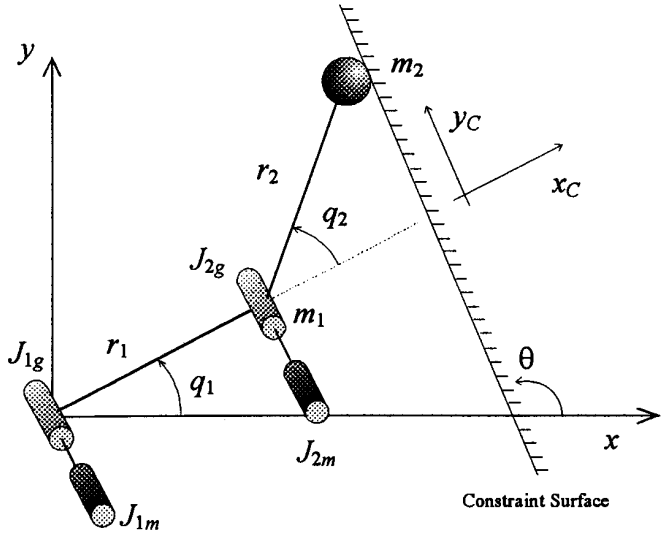

Figure 1: The 2R robot and the constraint surface.

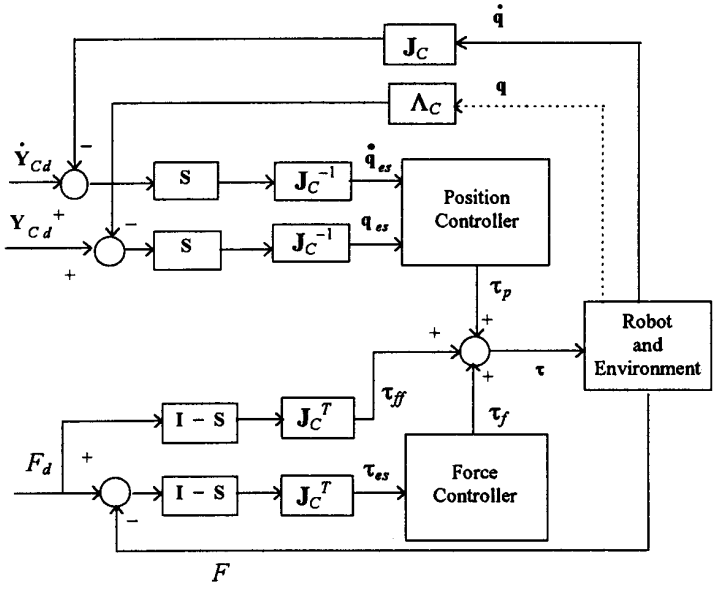

Figure 2: Block diagram of the position/force hybrid control algorithm.

3. SOME SIMULATION RESULTS

In this section we study the system response using VSCs, both at the position and force control loops (with a sampling frequency of $f_c = 10$ kHz), instead of the standard PID algorithms. The position/force controllers are the first-order VSCs (Azenha & Machado, 1996; Utkin, 1977) with a sliding surface and a control effort given by:

$$\mathbf{q}_{es}=\mathbf{J}_C^{-1}\mathbf{S}\left(\mathbf{Y}_{cd}-\mathbf{Y}_c\right),\ \sigma_i=\dot{q}_{esi}+c_{Pi}q_{esi} \tag{4a}$$

$$\tau_{VSCi} = \begin{cases} \tau_{Pmaxi} & ,\sigma_i \geq \tau_{Pmaxi} / K_{Pi} \\ K_{Pi}\sigma_i & ,|\sigma_i| < \tau_{Pmaxi} / K_{Pi} \\ -\tau_{Pmaxi} & ,\sigma_i \leq -\tau_{Pmaxi} / K_{Pi} \end{cases} \quad (4b)$$

$$\tau_{es} = \mathbf{J}_C^T(\mathbf{I}-\mathbf{S})(\mathbf{F}_d - \mathbf{F}), \ \sigma_i = \tau_{esi} + c_{Fi}\int \tau_{esi} dt \quad (4c)$$

$$\tau_{VSCi} = \begin{cases} \tau_{Fmaxi} & ,\sigma_i \geq \tau_{Fmaxi} / K_{Fi} \\ K_{Fi}\sigma_i & ,|\sigma_i| < \tau_{Fmaxi} / K_{Fi} \\ -\tau_{Fmaxi} & ,\sigma_i \leq -\tau_{Fmaxi} / K_{Fi} \end{cases} \quad (4d)$$

Table 2 shows the numerical values of the controllers adopted in this section. These parameters were tuned by trial and error and represent a compromise between fast transients and large overshoots.

Table 2: Numerical values of the First-order VSCs.

Joint i	K_{Pi}	K_{Fi}	τ_{Pmaxi}	τ_{Fmaxi}	c_{Pi}	c_{Fi}
1	10,000	100	1,000	1,000	2.5	0.25
2	10,000	100	500	500	2.5	0.25

In a first case study, the adopted constraint surface parameters are $M = 0$ Kg, $B = 1$ Ns/m, $K = 100$ N/m, $\theta = \pi/2$ and an initial operating point $q_{10} = q_{20} = \pi/2$, where q_{i0} stands for $q_i(t = 0)$, $i = 1,2$. In Fig. 3 we present the time response for a position input step ($\delta y_{Cd} = 0.1$ m) established at $t = 3$ to damp out the initial conditions. In Fig. 4 an alternative experiment, shows the time response for a force input step ($\delta F_d = 1$ N) at $t = 3$.

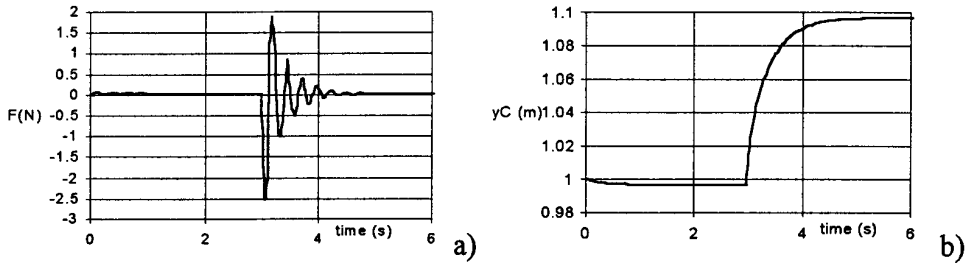

Figure 3: Time responses of the position/force hybrid control system for a step position input $\delta y_{Cd} = 0.1$ m (case study 1, $q_{10} = q_{20} = \pi/2$): a) Force; b) Position. $f_c = 10$ kHz.

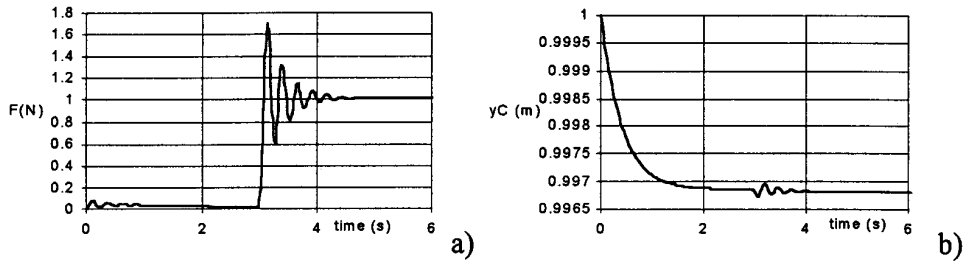

Figure 4: Time responses of the position/force hybrid control system for a step force input $\delta F_d = 1$ N (case study 1, $q_{10} = q_{20} = \pi/2$): a) Force; b) Position. $f_c = 10$ kHz.

In a second case study we introduce an integral term in the sliding surface of the position--VSC according with the equations:

$$\mathbf{q}_{es} = \mathbf{J}_C^{-1}\mathbf{S}(\mathbf{Y}_{cd} - \mathbf{Y}_c),\ \sigma_i = \dot{q}_{esi} + 2\omega_{ni}\xi_i q_{esi} + \omega_{ni}^2 \int q_{esi} dt \tag{5a}$$

$$\tau_{VSCi} = \begin{cases} \tau_{Pmaxi} & ,\sigma_i \geq \tau_{Pmaxi} / K_{Pi} \\ K_{Pi}\sigma_i & ,|\sigma_i| < \tau_{Pmaxi} / K_{Pi} \\ -\tau_{Pmaxi} & ,\sigma_i \leq -\tau_{Pmaxi} / K_{Pi} \end{cases} \tag{5b}$$

The parameters of the sliding surface are $\omega_{ni} = 7.91$ rads^{-1} and $\xi_i = 1.74$ ($i = 1,2$). By this way, the dominant eigenvalue of the sliding surface remains unchanged. This controller enables us to have small position errors, because of the integral action in the second order sliding surface. In this line of thought, Figs. 5 and 6 present the system time responses for the same test input signals. As can be seen in Figs. 3-4 and Figs. 5-6, for $\theta = \pi/2$ and , $q_{10} = q_{20} = \pi/2$, the second-order VSC in the position control loop leads to much smaller steady-state position errors, while the transient remains approximately the same.

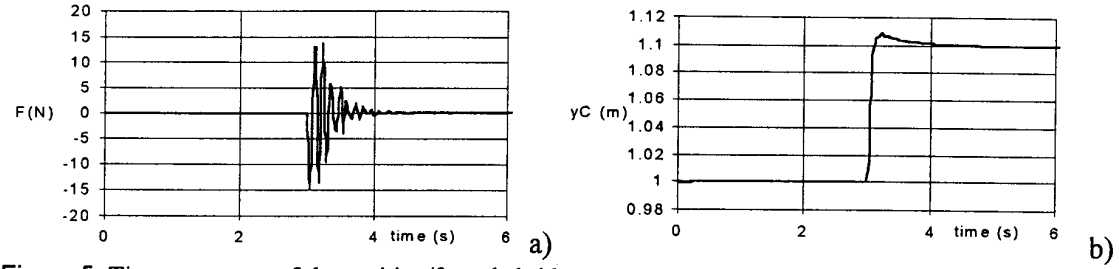

a) b)

Figure 5: Time responses of the position/force hybrid control system for a step position $\delta y_{Cd} = 0.1$ m (case study 2, $q_{10} = q_{20} = \pi/2$): a) Force; b) Position. $f_c = 10$ kHz.

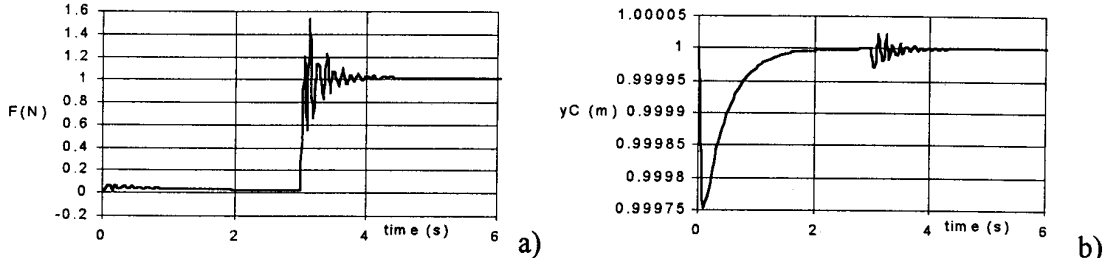

a) b)

Figure 6: Time responses of the position/force hybrid control system for a step force input $\delta F_d = 1$ N (case study 2, $q_{10} = q_{20} = \pi/2$): a) Force; b) Position. $f_c = 10$ kHz.

4. FREQUENCY RESPONSE OF THE SYSTEM

In this section we start by choosing a distinct operating point, because it is important to study the controller performance under different conditions. In this line of thought, in a third case study the initial parameters are $\theta = \pi/2$, $q_{10} = q_{20} = 15\pi/36$, $K = 100$ N/m, $B = 1$ Ns/m and $M = 0$ Kg (case study 3). Fig. 7 shows the corresponding *FRs* of the system for the first order VSCs with the parameters of Table 2, and two different amplitude input signals $\delta y_{Cd} = 0.03$ m or $\delta y_{Cd} = 0.1$ m and $\delta F_d = 1$ N or $\delta F_d = 4$ N.

The *FR* of the system for the case study 1 is nearly the same and, therefore, it is not presented. On the other hand, for the case study 2 we get a slightly different *FR* as can be seen in Fig. 8. Nevertheless, the overall characteristics remain almost unchanged revealing that the VSC-hybrid controller is robust against operating point variations. Moreover, from Figs. 7-8 we conclude that the *FR* has low sensitivity to variation of the amplitude of the reference signal, meaning that the closed-loop system has a behaviour such as a linear one. The low-pass

responses of $|Y_C/Y_{Cd}|$ and $|F/F_d|$ have a cut-off frequency that depends on the environment parameters. In particular, the resonance frequency f_0 of $|F/F_d|$ is very sensitive while $|Y_C/Y_{Cd}|$ has a much smaller sensitivity. In $|Y_C/F_d|$ and $|F/Y_{Cd}|$ we have bandpass *FRs* with resonance peaks located also at f_0.

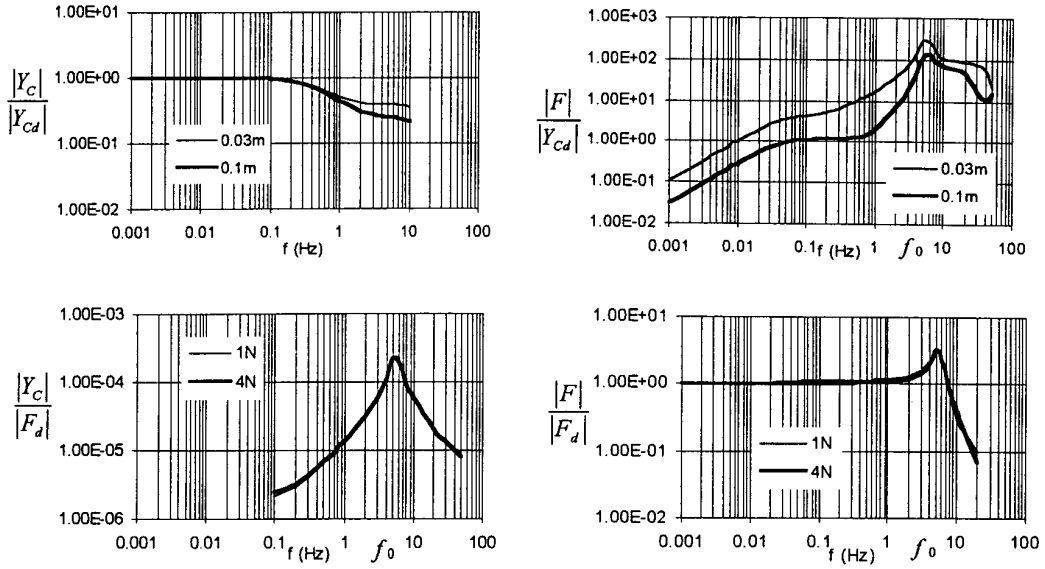

Figure 7: Frequency responses of the position/force hybrid VSC (case study 3, $q_{10} = q_{20} = 15\pi/36$). f_c = 10 kHz.

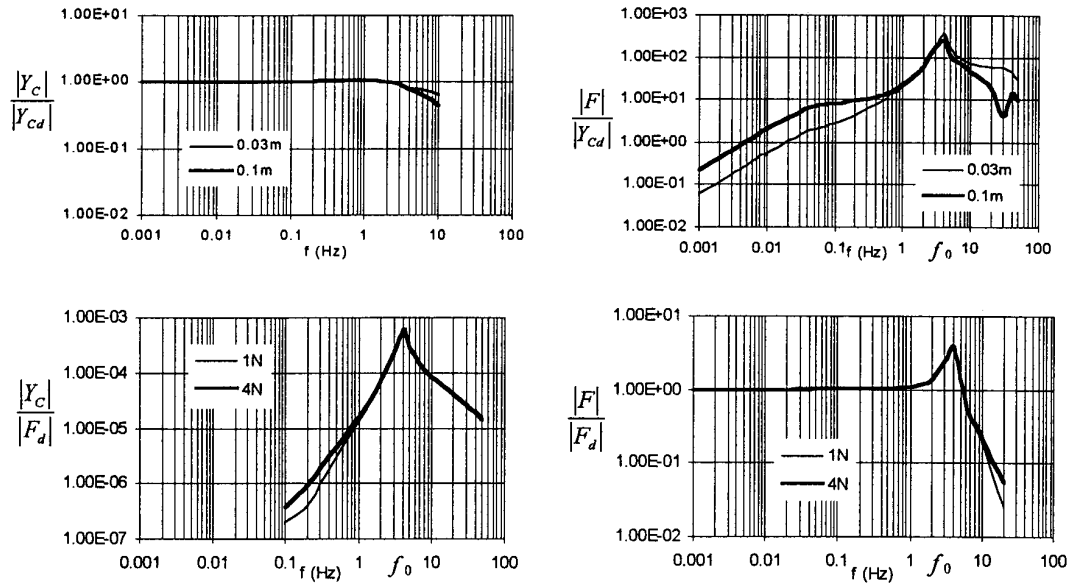

Figure 8: Frequency responses of the position/force hybrid VSC (case study 2, $q_{10} = q_{20} = \pi/2$). f_c = 10 kHz.

Another important system characteristic to study is the effect of the controller sampling frequency upon the system performances. The experiments showed that f_c = 10 kHz is a controller frequency that leads to good results. Nevertheless, for operating points with an high damping coefficient B it is found that lower frequencies up to f_c = 500 Hz are acceptable being the *FRs* almost identical.

5. STABILITY ANALYSIS THROUGH LINEARIZATION

In this section it is presented an analysis of the system stability through its linearization. Notice that, for analysing the system stability with large amplitude signals, in general we must employ the describing function (Atherton, 1975) instead of a simple linearization. Nevertheless, the observed limit cycles revealed small amplitudes and, therefore, the linearization method is sufficient.

The system equations can be simplified resulting the MIMO system equations:

$$\begin{bmatrix} Q_{1,\text{output}} \\ Q_{2,\text{output}} \end{bmatrix} = \begin{bmatrix} N_{11} & N_{12} \\ N_{21} & N_{22} \end{bmatrix} \begin{bmatrix} Q_{1,\text{input}} \\ Q_{2,\text{input}} \end{bmatrix} \tag{6}$$

where $Q_{i,\text{input}}$ and $Q_{i,\text{output}}$ stands for the Laplace transform of $q_{i,\text{input}}$ and $q_{i,\text{output}}$ ($i = 1,2$) and N_{ij} ($i, j = 1, 2$) represents the linearized transfer function between the input variable i and the output variable j. Then, setting $Q_{i,\text{input}} = Q_{i,\text{output}}$ we can apply the Nyquist multivariable criterion which leads to the characteristic equation:

$$N_{11}N_{22} - N_{11} - N_{22} - N_{12}N_{21} + 1 = 0 \tag{7}$$

For example, for $f_c = 10$ kHz and $\theta = \pi/2$, $q_{10} = q_{20} = 15\pi/36$, $K = 100$ N/m, $B = 0.03$ Ns/m and $M = 0$ Kg we find a limit cycle of 5 Hz that is in accordance with expression (7).

The Nyquist diagram of the system for several controller frequencies is shown in Fig. 9. It can be seen that for $f_c = 10$ kHz the limit cycle is stable while decreasing f_c the system becomes unstable.

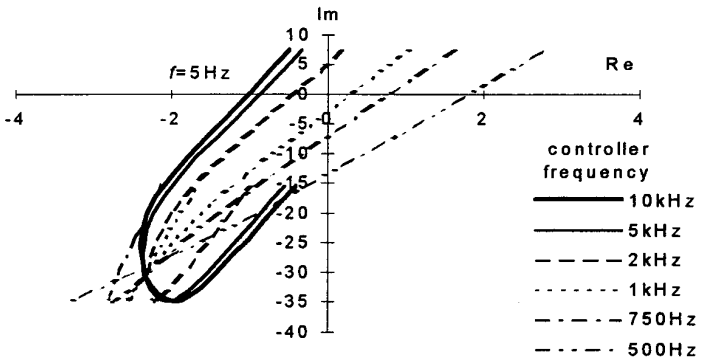

Figure 9: Nyquist diagram of the system for several controller frequencies.

In conclusion, the Nyquist diagram represents a useful tool for analysing the system stability.

6. CONCLUSIONS

This paper presented the design and implementation of position/force hybrid VSC of robot manipulators. Several controllers and operating conditions were studied and the second order VSC was shown to be superior because it reduced the steady-state position error. Frequency response techniques were also employed in the characterisation of system behaviour and good linearity properties were found. The stability and accuracy of the system are shown to be satisfactory and the influence of sampling frequency was investigated.

ACKNOWLEDGEMENT
This paper was developed under the grant PRAXIS XXI/BD/4524/94 from JNICT.

7. REFERENCES

AN, C. H. & J. M. HOLLERBACH, Kinematic Stability Issues in Force Control of Manipulators, *Proc. of the IEEE Int. Conf. on Robotics and Automation*, pp. 897-903, 1987.

ATHERTON, D. P., *Nonlinear Control Engineering*, Van Nostrand Reinhold Company, London, 1975.

AZENHA, A. & J. A. T. MACHADO, Variable Structure Control of Systems with Nonlinear Friction and Dynamic Backlash, *IFAC 13th World Congress*, San Francisco, California, USA, vol. E, pp. 515-520, 1996.

AZENHA, A. & J. A. T. MACHADO, Stability Analysis in Variable Structure Position/Force Hybrid Control of Manipulators, *IEEE International Conference on Intelligent Engineering Systems*, Budapest, Hungary, 1997.

FISHER, W. D. & M. S. MUJTABA, Sufficient Stability Condition for Hybrid Position/Force Control, *Proc. of the Int. Conf. on Rob. and Automation*, Nice, France, pp. 1336-1341, 1992.

HOGAN, N., Impedance Control: An Approach to Manipulation, Parts I-Theory, II--Implementation and III-Applications, *ASME Journal of Dynamic Systems, Measurement, and Control*, vol. 107, No. 1, pp. 1-24, 1985.

KHATIB, O., A Unified Approach for Motion and Force Control of Robot Manipulators: The Operational Space Formulation, *IEEE J. of Rob. and Autom.*, vol. 3, No. 1, pp. 43-53, 1987.

RAIBERT, M. H. & J. J. CRAIG, Hybrid Position/Force Control of Manipulators, *ASME Journal of Dynamic Systems, Measurement, and Control*, vol. 102, No. 2, pp. 126-133, 1981.

SICILIANO, B. & L. VILLANI, A Force/Position Regulator for Robot Manipulators Without Velocity Measurements, *IEEE Int. Conf. on Robotics and Automation*, Minneapolis, USA, pp. 2567-2572, 1996.

UTKIN, V. I., Variable Structure Systems With Sliding Modes, *IEEE Transactions on Automatic Control*, vol. 22, pp. 212-222,1977.

VOLPE, R. & P. KHOSLA, Computational Considerations in the Implementation of Force Control Strategies, *Journal of Intelligent and Robotic Systems*, vol. 9, pp. 121-148, 1994.

WHITNEY, D. E., Historical Perspective and State of the Art in Robot Force Control, *The Int. J. of Robotics Research*, vol. 6, No. 1, pp. 3-14, 1987.

ZHANG, H. & R. P. PAUL, Hybrid Control of Robot Manipulators, *Proc. of the IEEE Int. Conf. on Robotics and Automation*, USA, pp. 602-607, 1985.